Am J Clin Exp Urol 2020;8(1):18-27
www.ajceu.us /ISSN:2330-1910/AJCEU0108751

Original Article

EAF2 loss induces prostatic intraepithelial neoplasia from luminal epithelial cells in mice

Laura E Pascal[1], Lora H Rigatti[3], Junkui Ai[1], Aiyuan Zhang[1], Jianhua Zhou[1], Joel B Nelson[1], Zhou Wang[1,2,4]

Departments of [1]Urology, [2]Pharmacology and Chemical Biology, University of Pittsburgh School of Medicine, Pittsburgh, PA, USA; [3]Division of Laboratory Animal Resources, University of Pittsburgh School of Medicine, Pittsburgh, PA 15216, USA; [4]University of Pittsburgh Cancer Institute, University of Pittsburgh School of Medicine, Pittsburgh, PA, USA

Received February 5, 2020; Accepted February 18, 2020; Epub February 25, 2020; Published February 28, 2020

Abstract: Defining the cell of origin for prostatic carcinogenesis is fundamentally important for understanding the mechanisms leading to prostate cancer. Lineage tracing studies have demonstrated that luminal epithelial cells are capable of self-replication in multiple organs, including the adult murine prostate, and cell of prostate cancer origin studies have shown that while both the luminal and basal murine prostate epithelial cells are capable of neoplastic transformation, luminal cells are more efficient as the origin of prostate cancer. ELL-associated factor 2 (EAF2) is an androgen responsive tumor suppressive protein expressed by prostate luminal epithelial cells that is frequently down-regulated in primary prostate tumors. EAF2 knockdown induces prostate cancer cell proliferation and invasion *in vitro* and mice with *Eaf2* deficiency develop epithelial hyperplasia and murine prostatic intraepithelial neoplasia (mPIN) lesions. Here, we utilized an Eaf2 knockout, PSA-CreER^{T2} transgenic model crossed with a fluorescent reporter line to show that *Eaf2* deficiency induces mPIN lesions derived from the luminal cell lineage. These results suggest that PIN lesions in the Eaf2 knockout mouse were derived from prostate luminal epithelial cells, further suggesting that the prostatic luminal epithelial cell is the major origin of prostate carcinogenesis.

Keywords: EAF2, prostate cancer, lineage tracing, PSA-CreER^{T2}

Introduction

Prostate tumors are characterized by heterogeneity in their expression of luminal and basal epithelial phenotypes. Clinically localized tumors predominantly exhibit a more luminal epithelial phenotype including their expression of androgen receptor (AR) and prostate specific antigen (PSA), while loss of AR and PSA and gain of stem cell-like, less differentiated phenotypes have been associated with more aggressive disease [1-3]. Stratification of prostate cancer into low-risk or high-risk disease currently drives treatment selection, however a recent study suggests that overtreatment of low-risk and in particular, the undertreatment of high-risk prostate cancers is a persistent problem [4]. It has been proposed that identifying the cell of origin for prostate tumors could provide valuable insight into more effective stratification and treatment selection for patients.

Lineage analysis in murine models has proven to be a powerful tool for studying both prostate development [5, 6] and the maintenance of adult homeostasis [7, 8], as well as identifying the potential prostate cancer cell of origin [8-12]. Lineage studies have demonstrated that the basal and secretory luminal epithelial cells in the adult murine prostate are two independent self-sustained lineages [7, 8] and are both capable of neoplastic transformation in mice with prostate-specific *Pten* deletion [8-11]. Choi et al., showed that Pten deletion in either the prostate basal or luminal cells could initiate tumorigenesis and that prostate tumorigenesis in mice with basal cell *Pten* deletion had a longer latency than mice with luminal cell *Pten* deletion [8]. In a similar study also using the *Pten* knockout model, Wang et al., showed that tumors with a gene signature consistent with luminal origin prostate cancer were more likely to be high-risk than basal origin prostate can-

cer [11]. Another study utilized the murine *Pten* knockout model to show that basal-derived prostate cancers require β-catenin, while luminal-derived prostate tumors did not [10]. These studies have provided critical insights into the impact of cell of origin on prostate tumorigenesis and progression in tumors initiated by PTEN inactivation, however PTEN is not generally considered an initiating event in prostate tumorigenesis and there are multiple genetic alterations associated with prostate cancer. In an expanded analysis including Hi-*Myc*, TRAMP and T+E2 models in addition to the *Pten* model, lineage-tracing of basal and luminal tumorigenesis also showed that luminal cells were the favored cell of tumor origin in these other models [12]. This latter study's inclusion of the T+E2 model, where tumor initiation was induced after lineage marking, provided additional critical evidence that the luminal cell is much more sensitive to neoplastic transformation than the basal cell. However, comprehensive analysis of other genetically engineered models of prostate tumorigenesis will likely be essential for providing additional insights into the development and progression of prostate cancer.

EAF2 is an androgen-responsive gene that is frequently down-regulated in advanced prostate cancer [13, 14], and up-regulated in the epithelium of benign prostatic hyperplasia nodules [15]. EAF2 is expressed by luminal epithelial cells in the human prostate [13] as well as the mouse prostate [16]. Knockdown of EAF2 in prostate cancer cell lines has been shown to enhance proliferation, migration and invasion [17]. In murine models, homozygous *Eaf2* deficiency induced increased proliferation and induced high-grade murine prostatic intraepithelial neoplasia (mPIN) in multiple strains [14, 16, 18]. Cumulatively, these studies suggest that EAF2 has tumor suppressive properties in the prostate.

In the current study, the potential for luminal epithelial cells to develop into mPIN lesions in an *Eaf2*$^{-/-}$ mouse model was explored. Lineage tracing reporter mice with homozygous deficiency in *Eaf2* were generated and tamoxifen induced labeling was performed at 7 weeks of age. Mice were analyzed for histological defects at 12 months of age and labeling efficiency was determined.

Materials and methods

Generation of luminal epithelial lineage tracing Eaf2 deletion mice

The *Eaf2* conventional deletion mouse on a C57BL/6J background was generated as previously [19]. Genotyping was determined by PCR analysis of genomic mouse tail DNA and confirmed on muscle DNA when animals were euthanized as previously described for conventional deletion of *Eaf2* [18].

Lineage tracing mice were generated to determine whether prostatic intraepithelial neoplasia could be derived from luminal and/or basal epithelial cells in the previously described *Eaf2* knockout mouse model [14]. The breeding strategy first crossed the PSA-CreER^{T2} mouse [20] (a generous gift from Dr. Pierre Chambon and Dr. Daniel Metzger, Institute of Genetics and of Molecular & Cellular Biology, Strasbourg, France) with the *Eaf2*$^{-/-}$ mouse to generate PSA-CreER^{T2}; *Eaf2*$^{-/-}$ mice (Figure S1A). These mice were then crossed with the R26RmT/mG double-fluorescent Cre reporter mouse (Stock# 007676, The Jackson Laboratory) to generate PSA-CreER^{T2}; R26RmT/mG; *Eaf2*$^{-/-}$ mice on a C57BL6/J background (Figure S1B). All animal studies were reviewed and approved by the Institutional Animal Care and Use Committee (IACUC) of the University of Pittsburgh and were conducted in strict accordance with the standards for humane animal care and use as set by the Animal Welfare Act and the National Institutes of Health guidelines for the use of laboratory animals. All mice were maintained identically. Genotyping was determined by PCR analysis of genomic mouse tail DNA and confirmed on muscle DNA when animals were euthanized (Figure S2). Primers specific for Cre recombinase mice were upstream primer TTGCCTGCATTACCGGTCGATG and downstream primer TCCAGCCACCAGCTTGCATG. PCR for Cre recombinase was carried out at 94°C 2 min, 94°C, 30 s, 55°C 1 min, 72°C 30 s for 35 cycles, followed by 72°C 5 min, hold at 4°C. PCR for mT/mG was carried out as in our previous study [7].

Tamoxifen (TAM) induction of Cre activity in mice containing the PSA-CreER^{T2} allele was performed as previously described [7]. TAM suspended in 100 µl final volume Kolliphor at a concentration of 3 mg TAM/40 g body weight

Table 1. Labeling efficiency of luminal epithelial cells in PSA-CreER^{T2}; R26RmT/mG; Eaf2$^{-/-}$ control (-TAM) mice

Mouse ID	Image ID	Number of green (labeled) cells	Number of red cells	Total number of cells counted	Overall labeling efficiency (%)
a	a 1	14	67		
a	a 2	8	93		
a	a 3	9	61		
a	a 4	23	69		
Total a:		54	290	344	15.70
b	b 1	30	20		
b	b 4	12	26		
b	b 3	7	44		
b	b 2	0	37		
Total b:		49	127	176	27.84
c	c 3	5	37		
c	c 2	5	41		
c	c 1b	20	54		
c	c 4	14	47		
c	c 5	0	87		
Total c:		44	266	310	14.19
d	d 1	54	58		
d	d 2	27	51		
d	d 3	43	99		
d	d 4	0	61		
d	d 5	24	54		
Total d:		148	323	471	31.42
f	f 1	0	59		
f	f 2	22	57		
Total f:		22	116	138	15.94

(TAM and Kolliphor were both from Sigma Chemical Co., St. Louis, MO, USA) or vehicle control (100 µl Kolliphor) was injected i.p. daily for 5 consecutive days in adult mice (7 weeks of age). Mice were euthanized at 12 mos of age.

The lateral prostate lobes were dissected and fixed in 4% paraformaldehyde for 24 hours, followed by 30% sucrose until tissue no longer floated (1-3 days). Lobes were then cryoembedded in OCT compound (Sakura Finetek USA, Inc., Torrance, CA, USA) for cryosectioning. Cryosections (3-5 µm) were washed with PBS and mounted with Vectastain mounting media (Vector Laboratories, Burlingame, CA, USA). Sections were imaged with a Zeiss Axioplan 2 microscope (Carl Zeiss AG, Oberkochen, Germany) equipped with a Photometrics Coolsnap HQ monochrome camera (Roper Scientific Photometrics, Tucson, AZ) and NIS-Elements BR v 3.2 software (Nikon Instruments, Inc., Mellville, NY). All tissues were examined by a board-certified veterinary pathologist (LHR).

Quantification of mG-labeled cells in lateral prostates

The overall percentage of mG-labeled cells was scored manually from at least three sections of lateral prostate tissue per animal with at least five animals per group. Sections were imaged at 40× and all visibly distinguishable cells in each field were counted. The percentage of mG-labeled cells was determined by dividing the number of labeled cells by the total number of cells scored in each region.

Histopathologic analysis and quantification of mG-labeled cells in mPIN lesions

Identification of mPIN lesions was performed by a board-certified animal pathologist in a blinded fashion (LHR, V.M.D.). Lesions were identified as murine prostatic intraepithelial neoplasia (mPIN) per the criteria published by Shappell, et al. for scoring prostate lesions in transgenic mouse models [21]. mPIN identified in the PSA-CreER^{T2}; R26RmT/mG; *Eaf2*$^{-/-}$ mice ranged from low grade to high grade. Low grade lesions were characterized by glands lined by 1 to 3 layers of epithelial cells displaying minimal pleomorphism or hyperchromasia, slight nuclear enlargement with little atypia, infrequent mitosis, and essentially normal glandular profiles with only occasional hints of papillary epithelial proliferation [21]. High grade lesions were characterized by extensive intraglandular epithelial proliferation, formation of papillary or cribriform structures consisting of epithelial cells displaying significant nuclear atypia and hyperchromasia, cellular pleomorphism, and increased frequency of mitoses [21]. The number of mG-labeled cells was counted in each

Table 2. Labeling efficiency of luminal epithelial cells in PSA-CreER^{T2}; R26RmT/mG; Eaf2$^{-/-}$ (+TAM) mice

Mouse ID	Image ID	Number of green (labeled) cells	Number of red cells	Total number of cells counted	Labeling efficiency (%)
A	A 1	66	21		
A	A 2	143	6		
A	A 3	69	4		
Total A:		278	31	309	89.97
B	B 1	30	18		
B	B 2	74	12		
B	B 3	79	35		
B	B 4	139	41		
Total B:		322	106	428	75.23
C	C 1	136	0		
C	C 2	144	10		
C	C 3	132	24		
Total C:		412	34	446	92.38
D	D 1	112	38		
D	D 2	115	24		
D	D 3	58	19		
D	D 4	73	23		
D	D 5	38	78		
Total D:		396	182	578	68.51
E	E 1	40	66		
E	E 2	94	75		
E	E 3	35	0		
E	E 4	94	8		
Total E:		263	149	412	63.83
F	F 1	109	7		
F	F 2	101	31		
F	F 3	108	16		
		318	54	372	85.48
G	G 1	108	15		
G	G 2	145	3		
G	G 3	125	5		
		378	23	401	94.26
I	I 1	109	37		
I	I 2	84	8		
I	I 3	97	22		
		290	67	357	81.23
J	J 1	104	34		
J	J 2	81	34		
J	J 3	78	23		
J	J 4	137	0		
		400	91	491	81.47

mPIN lesion and quantified as a percentage of the total number of cells in each lesion.

Statistical analysis

Comparison between groups were calculated using the Student's t-test. A value of $P< 0.05$ was considered significant. GraphPad Prism version 6.07 was used for graphics (GraphPad Software, San Diego, CA, USA). Values are expressed as means ± S.D.

Results

Genetic lineage tracing of luminal epithelial cells in the adult Eaf2 knockout mouse prostate

We and others previously demonstrated that adult prostate luminal epithelial cells were capable of surviving androgen deprivation and self-replicating upon androgen stimulation in a murine lineage tracing model [7, 8]. Here, we crossed the PSA-CreER^{T2}; R26RmT/mG mouse with the Eaf2 knockout mouse to generate PSA-CreER^{T2}; R26RmT/mG; *Eaf2*$^{-/-}$ mice. The double-fluorescent mT/mG permitted the visualization of recombined and non-recombined cells in mPIN lesions that developed in the PSA-CreER^{T2}; R26RmT/mG; *Eaf2*$^{-/-}$ mice. At 12 mos of age, mice were euthanized and prostates were examined for overall labeling efficiency and the labeling composition of mPIN lesions that developed in the aged animals. All raw data for mice treated with vehicle alone (-TAM) were listed in **Table 1**, and raw data for mice treated with tamoxifen (+TAM) were listed in **Table 2**.

The number of labeled (mG) cells in serial sections of lateral prostate lobes was quantified in control (-TAM) and labeled (+TAM) mice and an average labeling efficiency for each animal was determined (**Tables 1**, **2**).

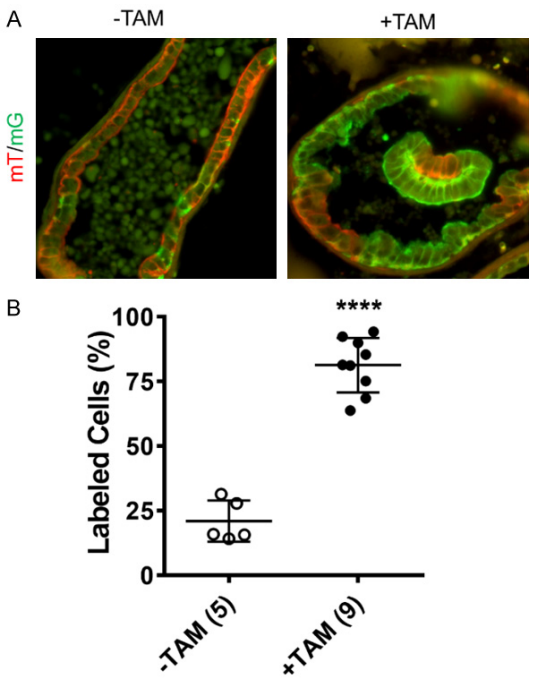

Figure 1. Visualization of recombined and non-recombined cells in the lateral prostate lobes of PSA-CreER^{T2}; R26RmT/mG; *Eaf2*$^{-/-}$ mice using fluorescence microscopy. A. Labeling efficiency in fixed tissue sections of 12 month old mice treated with vehicle control (-TAM) or tamoxifen (+TAM) at 7 weeks of age to induce transformation from mT (red) to mG (green) in luminal epithelial cells. B. Quantification of mG-labeled cells in -TAM and TAM mice at 12 months of age (at least 100 cells were counted for each mouse) as a percentage of the total number of cells in each field. Original magnification, ×40. Number of animals shown in parentheses. ****P<0.0001.

Control (-TAM) mice displayed an average of 21.02% spontaneous recombination at 12 mos of age (**Figure 1A**, left panel, & **1B**). Mice with tamoxifen induced recombination (+TAM) displayed an average 81.37% labeling (**Figure 1A**, right panel, & **1B**), which was consistent with our previous study utilizing the PSA-CreER^{T2}; R26RmT/mG mouse, suggesting that neither *Eaf2* deletion nor aging of the mice significantly impacted the labeling efficiency.

Genetic lineage tracing of luminal epithelial cells in the mPIN lesions of adult Eaf2 knockout mouse prostate

We have previously reported that *Eaf2*$^{-/-}$ mice have an increased incidence in prostate epithelial hyperplasia and mPIN without progression to invasive carcinoma in the C57BL/6J model [14, 16, 18, 22, 23]. Here, areas of mPIN were identified in both -TAM and +TAM mice by a board-certified animal pathologist (LHR) and the number of labeled cells in each lesion was quantified to determine the labeling efficiency for each individual mPIN lesion. All raw quantification data for mPIN lesions identified in mice treated with vehicle alone (-TAM) were listed in **Table 3**, and raw data for mice treated with tamoxifen (+TAM) were listed in **Table 4**. A total of 7 mPIN lesions were identified in the -TAM control mice, and a total of 32 mPIN lesions were identified in the +TAM mice. In mPIN lesions, the -TAM control mice displayed an average of 23.55% labeling efficiency, and the +TAM mice displayed an average labeling efficiency of 77.62% (**Figure 2**; **Tables 3**, **4**). The average labeling efficiency in the mPIN lesions for each group was similar and not significantly different to the overall labeling efficiency in that group (i.e., 21.02% overall vs. 23.55% in mPIN lesions, P=0.82 for control -TAM; and 81.37% overall vs. 77.62% in mPIN lesions, P=0.71 for +TAM).

The mPIN lesions in -TAM control mice were composed of either exclusively mT (red) or a mixture of mT and mG-labeled cells (mixed). Serial sectioning confirmed the lack of mG-labeled cells in the two mPIN lesions with 0% labeling (**Figure 3A**, left and center panels). The majority (5/7) of the mPIN lesions identified in the -TAM control mice displayed a mixed labeling phenotype (**Figure 3A**, right panel), ranging from 13.73-66.67% labeled cells (**Table 3**). The mPIN lesions in +TAM mice were composed of either a mixture or exclusively mG (green) labeled cells. None of the mPIN lesions identified in +TAM mice displayed 0% labeling. The mPIN lesions in +TAM mice ranged from 5.77% labeling to 100%. Many of the mPIN lesions displayed a mixed phenotype of labeled and unlabeled cells (17/32, 53.13%), while 46.88% (15/32) of the +TAM mice displayed mPIN lesions composed entirely of labeled cells.

The total number of cells in each mPIN lesion was not correlated with the efficiency of labeling (data not shown, P=0.22).

Discussion

In the current study, we examined the lineage of mPIN lesions in aged *Eaf2* knockout mice crossed with the PSA-CreER^{T2}; R26RmT/mG mouse. In agreement with previous lineage

Table 3. Labeling efficiency of luminal epithelial cells in mPIN lesions of PSA-CreER^{T2}; R26RmT/mG; Eaf2$^{-/-}$ control (-TAM) mice

Mouse ID	Image ID	Histological defects (# PIN lesions)	Number of green (labeled) cells	Number of red cells	Total number of cells counted	mPIN labeling efficiency (%)
a	a 1	1	12	31	43	27.91
a	a 4	1	23	69	92	25.00
b	b 4	1	12	26	38	31.58
b	b 3	1	7	44	51	13.73
b	b 2	1	0	37	37	0.00
d	d 1	1	48	24	72	66.67
d	d 4	1	0	42	42	0.00
	Total mPIN:	7			Average:	23.55

Table 4. Labeling efficiency of luminal epithelial cells in mPIN lesions of PSA-CreER^{T2}; R26RmT/mG; Eaf2$^{-/-}$ (+TAM) mice

Mouse ID	Image ID	Histological defects (# PIN lesions)	Number of green (labeled) cells	Number of red cells	Total number of cells counted	Labeling efficiency (%)
A	A 1	1	46	21	67	68.66
A	A 2	1	20	0	20	100.00
A	A 3	1	30	0	30	100.00
B	B 2	2 (right)	47	2	49	95.92
B	B 2	2 (left)	27	0	27	100.00
B	B 3	1	49	0	49	100.00
B	B 4	1	100	12	112	89.29
C	C 1	1	25	0	25	100.00
C	C 2	1	31	0	31	100.00
C	C 3	1	8	9	17	47.06
D	D 1	1	31	3	34	91.18
D	D 4	1	56	19	75	74.67
D	D 5	2 (right)	11	53	64	17.19
D	D 5	2 (left)	13	8	21	61.90
E	E 1	1	3	49	52	5.77
E	E 2	2 (right)	9	8	17	52.94
E	E 2	2 (left)	3	46	49	6.12
E	E 3	1	35	0	35	100.00
E	E 4	1	43	0	43	100.00
F	F 1	1	28	0	28	100.00
F	F 2	2 (upper)	32	0	32	100.00
F	F 2	2 (lower)	16	16	32	50.00
F	F 3	1	21	0	21	100.00
G	G 1	1	64	0	64	100.00
G	G 2	1	25	0	25	100.00
I	I 2	1	35	2	37	94.59
I	I 3	1	9	6	15	60.00
J	J 1	2 (right)	9	16	25	36.00
J	J 1	2 (left)	28	0	28	100.00
J	J 2	1	21	9	30	70.00
J	J 3	1	15	9	24	62.50
J	J 4	1	14	0	14	100.00
	Total mPIN:	32			Average:	77.62

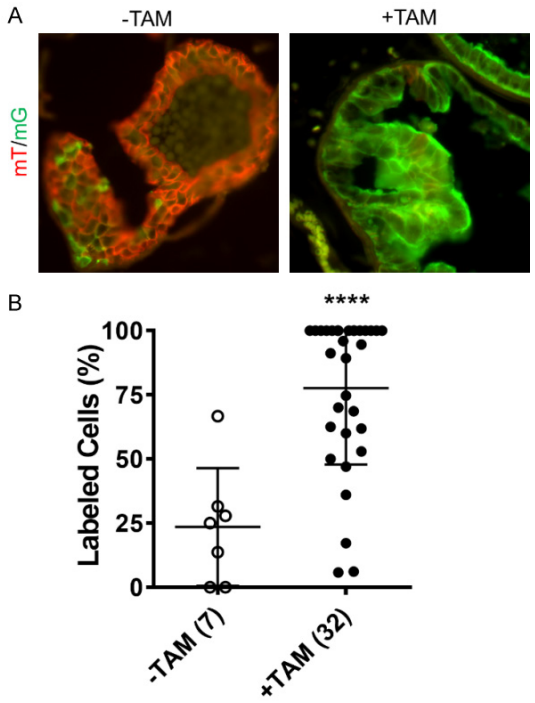

Figure 2. Labeling efficiency of mPIN lesions in the lateral prostate lobe of PSA-CreER^{T2}; R26RmT/mG; *Eaf2*$^{-/-}$ mice. A. Labeling efficiency in mPIN lesions in 12 month old mice treated with vehicle control (-TAM) or tamoxifen (+TAM) at 7 weeks of age to induce transformation from mT (red) to mG (green) in luminal epithelial cells. B. Quantification of mG-labeled cells in mPIN lesions of -TAM and TAM mice at 12 months of age as a percentage of the total number of cells in each mPIN lesion. mPIN lesions were identified by a board-certified veterinary pathologist (LHR). Original magnification, ×40. Number of mPIN lesions analyzed shown in parentheses, total number of animals was 5 -TAM and 9 +TAM mice. ****P<0.0001.

tracing studies in mice with other genetic defects [8-12], labeled mG luminal epithelial cells were capable of generating mPIN lesions in the Eaf2 knockout mouse model. The mPIN lesions in mG-labeled Eaf2 knockout mice were composed of either a mixture of labeled cells or were composed entirely of labeled cells, while mPIN lesions in vehicle control mice were composed entirely of unlabeled cells (mT) or were composed of approximately 24% spontaneously labeled mG cells. The overall labeling efficiency in both groups was similar to the labeling efficiency in mPIN lesions. Labeling of cells in control -TAM mice was specific to luminal cells, indicating the CreER expression was responsible for the labeling in the controls. The spontaneous recombination observed in the -TAM mice should not affect the data interpretation because TAM-induced very efficient labeling and the difference between controls and treated animals was statistically significant.

Overall labeling efficiency in the +TAM group was 81.37%, which was not significantly different from the labeling efficiency in mPIN lesions from this group (77.62%, P=0.64) and was also consistent with the labeling efficiency reported in our previous study in PSA-CreER^{T2}; R26RmT/mG mice at younger ages (~70%) [7]. This similarity in labeling efficiency, coupled with the absence of mPIN lesions composed entirely of non-labeled cells in mG-labeled *Eaf2* knockout mice suggests that in mice with *Eaf2* loss, mPIN lesions are mainly derived exclusively from luminal cells. However, this study does not directly address if mPIN lesions can be derived from basal cells in Eaf2 knockout mice, which is a limitation of using PSA-CreER^{T2} inducible knockout strategy to label luminal epithelial cells. Regardless, our findings are in agreement with the previous findings in the PTEN knockout models that basal cells were more resistant to malignant transformation than luminal cells [8], and that while basal-to-luminal cell differentiation is possible, it is an infrequent event in the adult prostate [8, 11]. This also is supportive of our previous studies of clinical prostate tumor specimens showing that localized primary prostate tumors displayed a luminal phenotype and the loss of differentiation in more advanced prostate tumors was not associated with a more basal like phenotype [1]. Another group also showed that cultured tumor cells from clinical specimens displayed a luminal/secretory phenotype [3].

The finding of mixed populations of labeled and unlabeled cells in about half of mPIN lesions in +TAM Eaf2 knockout mice suggests that PIN lesions can be derived from different adjacent luminal epithelial cells. The observation of mPIN lesions composed entirely of labeled cells could be due to the development of mPIN lesions from several cells, or from one transformed cell. However, the absence of mPIN lesions composed entirely of unlabeled cells and the preponderance of segregated groups of labeled and unlabeled cells in the +TAM group suggests that the expansion of luminal epithelial cells in mPIN lesions can be driven by proliferative expansion of one cell as well as a group of cells proliferating at the same time.

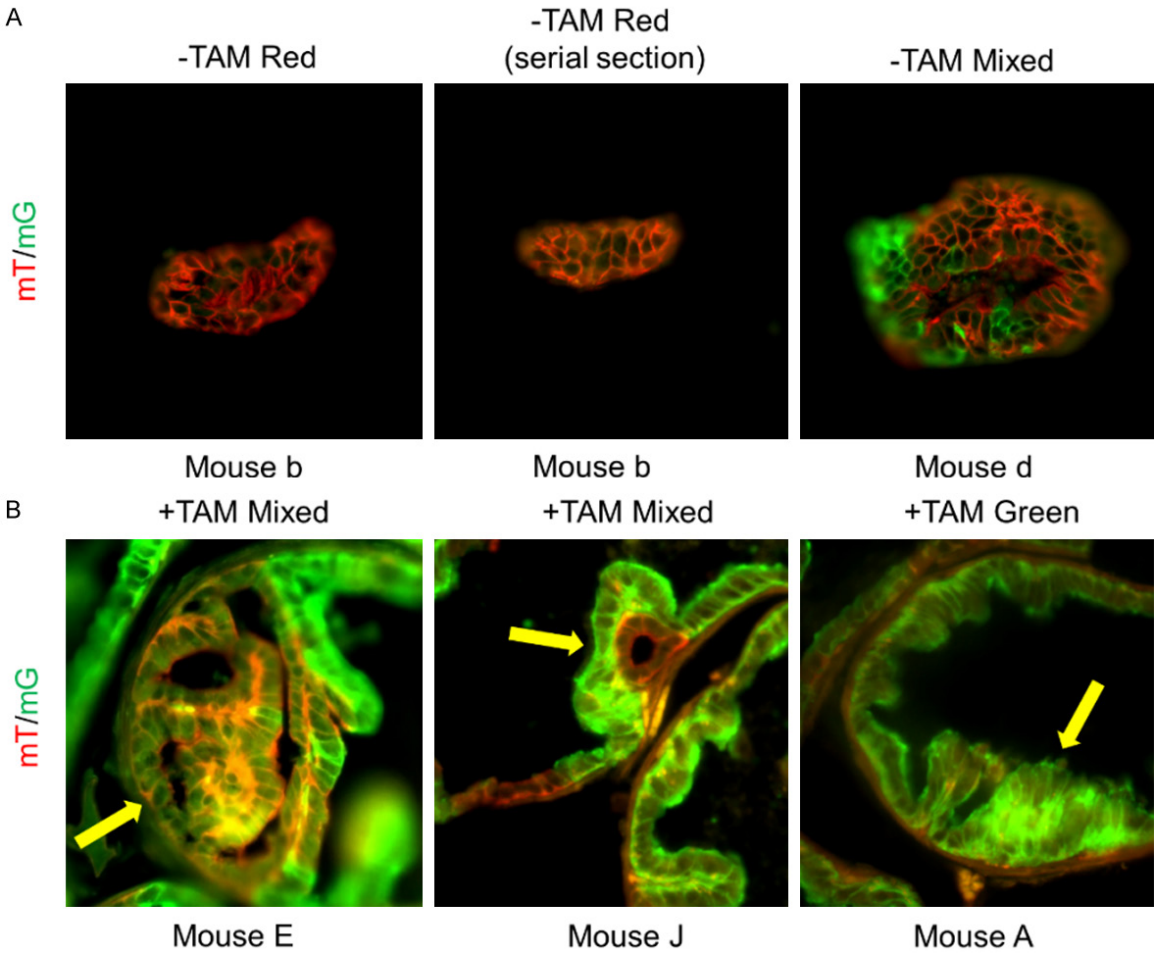

Figure 3. Labeling composition of mPIN lesions in the lateral prostate lobe of PSA-CreER^{T2}; R26RmT/mG; *Eaf2*$^{-/-}$ mice. A. mPIN lesions in 12 month old mice treated with vehicle control (-TAM) were composed entirely of either unlabeled mT cells (left and center panel), or a mixture (Mixed) of mG-labeled cells and mT cells (right panel). B. mPIN lesions (yellow arrows) in +TAM mice were composed of either Mixed or entirely mG-labeled cells (Green). mPIN lesions were identified by a board-certified veterinary pathologist (LHR). Original magnification, ×40.

Although it is not clear if human PIN and prostate tumors can also be derived similarly, many studies have reported that clinical prostate cancer is often composed of multiple distinct foci of independent origin with varying metastatic potential [24-28]. Conventional deletion of Eaf2 also does not preclude the possibility that neoplastic transformation could occur prior to adulthood and thus prior to labeling in this model. However, our findings are in agreement with the T+E2 lineage tracing model which found that even when labeling was performed prior to prostate tumor initiation, tumors were derived from luminal cells [12]. Lineage tracing studies can thus provide a powerful tool for determining if these differences are driven by genomic changes subsequent to neoplastic transformation or if they are driven by the original lineage of the transformed cell.

Our data suggest that luminal epithelial cells are the major cells of origin for mPIN lesions in the Eaf2 knockout mouse model, further substantiating the role of luminal epithelial cells as cells of origin for prostate cancer.

Acknowledgements

We are grateful to Dr. Pierre Chambon and Dr. Daniel Metzger for their generous gift of the PSA-CreERT2 mouse and Robin Frederick and Megan Lambert for technical support. This work was funded in part by the DoD grant W81XWH-12-1-0247 (J.B.N.), National Institutes of Health Grants R01 CA186780 (Z.W.), R50 CA211242 (L.E.P.). This project used the UPCI Hillman Cancer Center Animal Facility and was supported in part by award P30 CA047904.

Disclosure of conflict of interest

None.

Address correspondence to: Zhou Wang, University of Pittsburgh Cancer Institute, University of Pittsburgh School of Medicine, Pittsburgh, PA, USA. E-mail: wangz2@upmc.edu

References

[1] Pascal LE, Vencio RZ, Vessella RL, Ware CB, Vencio EF, Denyer G and Liu AY. Lineage relationship of prostate cancer cell types based on gene expression. BMC Med Genomics 2011; 4: 46.

[2] Mapelli SN, Albino D, Mello-Grand M, Shinde D, Scimeca M, Bonfiglio R, Bonanno E, Chiorino G, Garcia-Escudero R, Catapano CV and Carbone GM. A novel prostate cell type-specific gene signature to interrogate prostate tumor differentiation status and monitor therapeutic response (running title: phenotypic classification of prostate tumors). Cancers (Basel) 2020; 12.

[3] Nanni S, Priolo C, Grasselli A, D'Eletto M, Merola R, Moretti F, Gallucci M, De Carli P, Sentinelli S, Cianciulli AM, Mottolese M, Carlini P, Arcelli D, Helmer-Citterich M, Gaetano C, Loda M, Pontecorvi A, Bacchetti S, Sacchi A and Farsetti A. Epithelial-restricted gene profile of primary cultures from human prostate tumors: a molecular approach to predict clinical behavior of prostate cancer. Mol Cancer Res 2006; 4: 79-92.

[4] Cooperberg MR, Broering JM and Carroll PR. Time trends and local variation in primary treatment of localized prostate cancer. J Clin Oncol 2010; 28: 1117-1123.

[5] Ousset M, Van Keymeulen A, Bouvencourt G, Sharma N, Achouri Y, Simons BD and Blanpain C. Multipotent and unipotent progenitors contribute to prostate postnatal development. Nat Cell Biol 2012; 14: 1131-1138.

[6] Tika E, Ousset M, Dannau A and Blanpain C. Spatiotemporal regulation of multipotency during prostate development. Development 2019; 146.

[7] Liu J, Pascal LE, Isharwal S, Metzger D, Ramos Garcia R, Pilch J, Kasper S, Williams K, Basse PH, Nelson JB, Chambon P and Wang Z. Regenerated luminal epithelial cells are derived from preexisting luminal epithelial cells in adult mouse prostate. Mol Endocrinol 2011; 25: 1849-1857.

[8] Choi N, Zhang B, Zhang L, Ittmann M and Xin L. Adult murine prostate basal and luminal cells are self-sustained lineages that can both serve as targets for prostate cancer initiation. Cancer Cell 2012; 21: 253-265.

[9] Kwon OJ, Zhang L and Xin L. Stem cell antigen-1 identifies a distinct androgen-independent murine prostatic luminal cell lineage with bipotent potential. Stem Cells 2016; 34: 191-202.

[10] Lu TL and Chen CM. Differential requirements for beta-catenin in murine prostate cancer originating from basal versus luminal cells. J Pathol 2015; 236: 290-301.

[11] Wang ZA, Mitrofanova A, Bergren SK, Abate-Shen C, Cardiff RD, Califano A and Shen MM. Lineage analysis of basal epithelial cells reveals their unexpected plasticity and supports a cell-of-origin model for prostate cancer heterogeneity. Nat Cell Biol 2013; 15: 274-283.

[12] Wang ZA, Toivanen R, Bergren SK, Chambon P and Shen MM. Luminal cells are favored as the cell of origin for prostate cancer. Cell Rep 2014; 8: 1339-1346.

[13] Xiao W, Zhang Q, Jiang F, Pins M, Kozlowski JM and Wang Z. Suppression of prostate tumor growth by U19, a novel testosterone-regulated apoptosis inducer. Cancer Res 2003; 63: 4698-4704.

[14] Ai J, Pascal LE, O'Malley KJ, Dar JA, Isharwal S, Qiao Z, Ren B, Rigatti LH, Dhir R, Xiao W, Nelson JB and Wang Z. Concomitant loss of EAF2/U19 and Pten synergistically promotes prostate carcinogenesis in the mouse model. Oncogene 2014; 33: 2286-94.

[15] O'Malley KJ, Dhir R, Nelson JB, Bost J, Lin Y and Wang Z. The expression of androgen-responsive genes is up-regulated in the epithelia of benign prostatic hyperplasia. Prostate 2009; 69: 1716-1723.

[16] Pascal LE, Ai J, Masoodi KZ, Wang Y, Wang D, Eisermann K, Rigatti LH, O'Malley KJ, Ma HM, Wang X, Dar JA, Parwani AV, Simons BW, Ittman MM, Li L, Davies BJ and Wang Z. Development of a reactive stroma associated with prostatic intraepithelial neoplasia in EAF2 deficient mice. PLoS One 2013; 8: e79542.

[17] Ai J, Pascal LE, Wei L, Zang Y, Zhou Y, Yu X, Gong Y, Nakajima S, Nelson JB, Levine AS, Lan L and Wang Z. EAF2 regulates DNA repair through Ku70/Ku80 in the prostate. Oncogene 2017; 36: 2054-2065.

[18] Xiao W, Zhang Q, Habermacher G, Yang X, Zhang AY, Cai X, Hahn J, Liu J, Pins M, Doglio L, Dhir R, Gingrich J and Wang Z. U19/Eaf2 knockout causes lung adenocarcinoma, B-cell lymphoma, hepatocellular carcinoma and prostatic intraepithelial neoplasia. Oncogene 2008; 27: 1536-1544.

[19] Su F, Pascal LE, Xiao W and Wang Z. Tumor suppressor U19/EAF2 regulates thrombospondin-1 expression via p53. Oncogene 2010; 29: 421-431.

[20] Ratnacaram CK, Teletin M, Jiang M, Meng X, Chambon P and Metzger D. Temporally controlled ablation of PTEN in adult mouse pros-

tate epithelium generates a model of invasive prostatic adenocarcinoma. Proc Natl Acad Sci U S A 2008; 105: 2521-2526.

[21] Shappell SB, Thomas GV, Roberts RL, Herbert R, Ittmann MM, Rubin MA, Humphrey PA, Sundberg JP, Rozengurt N, Barrios R, Ward JM and Cardiff RD. Prostate pathology of genetically engineered mice: definitions and classification. The consensus report from the Bar Harbor meeting of the mouse models of human cancer consortium prostate pathology committee. Cancer Res 2004; 64: 2270-2305.

[22] Wang Y, Pascal LE, Zhong M, Ai J, Wang D, Jing Y, Pilch J, Song Q, Rigatti LH, Graham LE, Nelson JB, Parwani AV and Wang Z. Combined loss of EAF2 and p53 induces prostate carcinogenesis in male mice. Endocrinology 2017; 158: 4189-4205.

[23] Pascal LE, Ai J, Rigatti LH, Lipton AK, Xiao W, Gnarra JR and Wang Z. EAF2 loss enhances angiogenic effects of Von Hippel-Lindau heterozygosity on the murine liver and prostate. Angiogenesis 2011; 14: 331-343.

[24] Villers A, McNeal JE, Freiha FS and Stamey TA. Multiple cancers in the prostate. Morphologic features of clinically recognized versus incidental tumors. Cancer 1992; 70: 2313-2318.

[25] Boutros PC, Fraser M, Harding NJ, de Borja R, Trudel D, Lalonde E, Meng A, Hennings-Yeomans PH, McPherson A, Sabelnykova VY, Zia A, Fox NS, Livingstone J, Shiah YJ, Wang J, Beck TA, Have CL, Chong T, Sam M, Johns J, Timms L, Buchner N, Wong A, Watson JD, Simmons TT, P'ng C, Zafarana G, Nguyen F, Luo X, Chu KC, Prokopec SD, Sykes J, Dal Pra A, Berlin A, Brown A, Chan-Seng-Yue MA, Yousif F, Denroche RE, Chong LC, Chen GM, Jung E, Fung C, Starmans MH, Chen H, Govind SK, Hawley J, D'Costa A, Pintilie M, Waggott D, Hach F, Lambin P, Muthuswamy LB, Cooper C, Eeles R, Neal D, Tetu B, Sahinalp C, Stein LD, Fleshner N, Shah SP, Collins CC, Hudson TJ, McPherson JD, van der Kwast T and Bristow RG. Spatial genomic heterogeneity within localized, multifocal prostate cancer. Nat Genet 2015; 47: 736-745.

[26] Ruijter ET, van de Kaa CA, Schalken JA, Debruyne FM and Ruiter DJ. Histological grade heterogeneity in multifocal prostate cancer. Biological and clinical implications. J Pathol 1996; 180: 295-299.

[27] Bostwick DG, Shan A, Qian J, Darson M, Maihle NJ, Jenkins RB and Cheng L. Independent origin of multiple foci of prostatic intraepithelial neoplasia: comparison with matched foci of prostate carcinoma. Cancer 1998; 83: 1995-2002.

[28] Shoag J and Barbieri CE. Clinical variability and molecular heterogeneity in prostate cancer. Asian J Androl 2016; 18: 543-548.

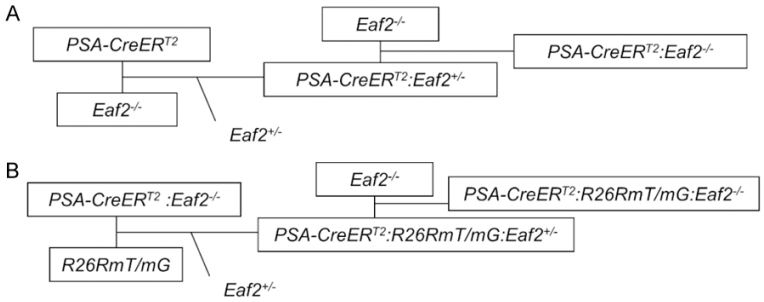

Figure S1. Breeding scheme used to generate (A) PSA-CreER^{T2}: Eaf2$^{-/-}$ mice and (B) PSA-CreER^{T2}: R26RmT/mG: Eaf2$^{-/-}$ mice.

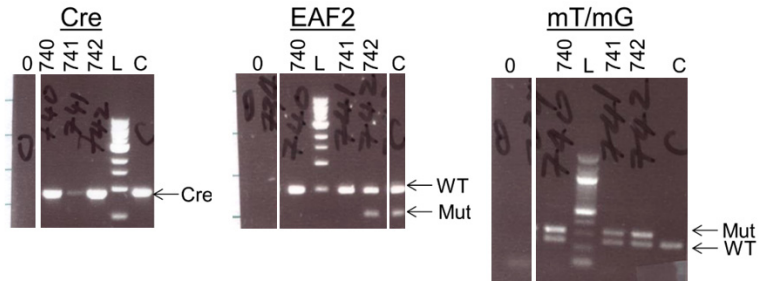

Figure S2. Genotypic analysis of offspring from PSA-CreER^{T2}; EAF2$^{-/-}$ mated to R26RmT/mG mice. Tail DNA was isolated from offspring at weaning and examined by PCR. Animal #742 is PSA-CreER^{T2}; R26RmT/mG; EAF2$^{+/-}$. Molecular weight ladders are shown (L) as well as negative (0) and positive controls (C). White space between gel images indicates where image was cut to show results from two non-consecutive lanes.